The Effect of Sterols on Amphotericin B Self-Aggregation in a Lipid Bilayer as Revealed by Free Energy Simulations

Anna Neumann,[†] Maciej Baginski,[†] Szymon Winczewski,[‡] and Jacek Czub[§*]
[†]Department of Pharmaceutical Technology and Biochemistry, [‡]Department of Solid State Physics, and [§]Department of Physical Chemistry, Gdansk University of Technology, Gdansk, Poland

ABSTRACT Amphotericin B (AmB) is an effective but toxic antifungal drug, known to increase the permeability of the cell membrane, presumably by assembling into transmembrane pores in a sterol-dependent manner. The aggregation of AmB molecules in a phospholipid bilayer is, thus, crucial for the drug's activity. To provide an insight into the molecular nature of this process, here, we report an atomistic molecular dynamics simulation study of AmB head-to-head dimerization in a phospholipid bilayer, a possible early stage of aggregation. To compare the effect of sterols on the thermodynamics of aggregation and the architecture of the resulting AmB-AmB complexes, free energy profiles for the dimerization in ergosterol- or cholesterol-containing and sterol-free membranes are derived from the simulations. These profiles demonstrate that although AmB dimers are formed in all the systems studied, they are significantly less favorable in the bilayer with ergosterol than in the cholesterol-containing or sterol-free ones. We investigate the structural and energetic determinants of this difference and discuss its consequences for the AmB mechanism of action.

INTRODUCTION

Amphotericin B (AmB, Fig. 1 *A*) is a potent polyene antibiotic used to treat systemic mycoses (1,2). It was introduced into clinical use in the 1960s and, despite its severe toxicity, remains an important antifungal drug in wide use today. Unfortunately, the rational design of the less toxic derivatives of AmB is hampered by the fact that its mechanism of action at the molecular level, although intensively studied, remains largely unknown.

AmB is known to increase the permeability of the cell membrane, presumably by assembling into transmembrane pores, which results in a disturbance of physiological ion transport and eventually leads to cell death (see reviews (3,4)). The presence of sterols in the membrane is important for the membrane-permeabilizing activity of the antibiotic; namely, at usual therapeutic concentrations (~10^{-6} M), increased ion flux is observed across the AmB-treated sterol-containing membranes and not across sterol-free ones (3,5). The chemotherapeutic activity of AmB, i.e., its selective toxicity for fungal cells, is due to the fact that AmB is more effective in permeabilizing fungal cell membranes with ergosterol (Erg, Fig. 1 *B*) than mammalian membranes with cholesterol (Cho, Fig. 1 *C*) (6,7). Also, it has been suggested that the membrane sterols affect the antifungal action of AmB either directly, by specifically binding to AmB molecules, or, indirectly, by modifying the structural and dynamic properties of the lipid bilayer. In the former case, the selective targeting of fungal membranes would be due to the stronger affinity of AmB for Erg than for Cho (8–10). It has been proposed, that the formation of specific complexes with sterols may be a necessary step for the assembly of AmB molecules into a functional transmembrane channel (11). Recently, it has also been reported that the specific Erg binding by AmB may cause sterol depletion, and thus, may itself be responsible for the fungicidal activity of the antibiotic, independent of membrane perforation (12,13).

In the indirect scenario, the sterol-containing membrane or membrane domain provides an appropriate lipid environment for the expression of the membrane-permeabilizing activity of AmB (14–18). Indeed, Erg and Cho are known for their ability to induce a so-called liquid-ordered phase, which is characterized by a higher conformational order of the lipid chains than the liquid-disordered phase in sterol-free membranes (19,20). Here, the selective toxicity for fungal membranes would be attributed to the stronger ordering effect of Erg on saturated phospholipids (19,21,22), which are known to be involved in the formation of the ordered domains (interestingly, it was found that Cho is more effective in ordering unsaturated lipids (19)). It is also important to note that under certain conditions the permeabilizing effects of AmB are also observed in sterol-free membranes, either at relatively high concentrations of the antibiotic, at low temperatures, or in the temperature-induced gel phase (7,14,15,23). Because AmB is known to induce order in sterol-free bilayers (24–26), AmB concentrations and temperature may also influence AmB activity in an indirect way, by modifying properties of the lipid bilayer.

It is widely accepted that the amphiphilic AmB molecules, when present in a lipid bilayer, can form the channel structures with their polar polyol chains lining the pore lumen and the hydrophobic polyene fragments exposed to the membrane hydrocarbon core. According to the classic barrel-stave channel model, sterol molecules directly

Submitted November 30, 2012, and accepted for publication February 20, 2013.

*Correspondence: jacczub@pg.gda.pl

Editor: Scott Feller.

0006-3495/13/04/1485/10 $2.00

http://dx.doi.org/10.1016/j.bpj.2013.02.029

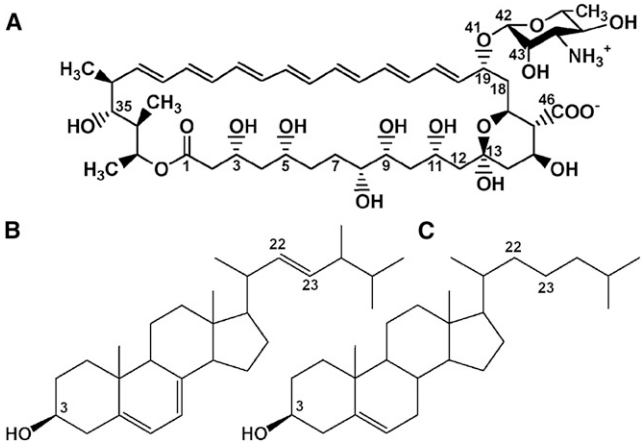

FIGURE 1 Chemical structure of the AmB (*A*), cholesterol (*B*), and ergosterol (*C*) molecules. The sugar moiety (mycosamine) and the carboxyl group form the so-called polar head of the AmB molecule.

participate in the channel formation (11), although, as mentioned above, it is now apparent that it is not always the case. The functional channels are proposed to be formed either by AmB-sterol complexes, AmB monomers, or self-aggregates (11,14,15,27). Before aggregation, these AmB species were found to adopt the orientation perpendicular to the membrane plane or to be in equilibrium between the perpendicular and the parallel orientation (28–30).

It is known that AmB aggregation in a phospholipid bilayer plays a major role in the membrane-disruptive activity of the antibiotic (3). In particular, the induction of increased membrane permeability is correlated with the detection of associated species of AmB (6). Differences in the thermodynamics of aggregation and in the architecture of the resulting AmB assemblies between membranes of a different sterol composition may determine the selectivity of the drug. Therefore, to test this idea, several studies have focused on the properties of the AmB dimerization process as a possible early stage of aggregation. AmB dimers have been investigated by fluorescence spectroscopy (molecular organization of AmB in solution and in lipid membranes (30,31)), by solid-state NMR (activity and geometry of covalently bound dimers, synthesized between two nonlabeled or isotopically labeled AmB molecules, in lipid membranes (32,33)) and theoretically (AmB dimers in vacuum and in water solution (34,35)). Generally, two relative arrangements of AmB molecules in the dimer are proposed: the parallel (head-to-head) orientation (with AmB polar heads interacting), and the antiparallel (head-to-tail) orientation. The head-to-head orientation has been recently proposed to be predominant in sterol-containing membranes (36). Nevertheless, despite numerous efforts, the molecular structure and energetics of self-assembled AmB dimers within the membrane environment have remained largely unexplored.

Here, we report molecular dynamics simulations performed to examine in atomic detail the parallel (head-to-head) dimerization of AmB in a phospholipid membrane. In particular, we present free energy profiles for the self-assembly of two antibiotic molecules embedded within a lipid bilayer determined using the so-called adaptive biasing force method (37,38). To enable a direct comparison of the effect of the lipid environment on the dimerization process, the free energy profiles were obtained for three different lipid membranes that are relevant to the biological activity of the antibiotic (Erg- and Cho-containing DMPC bilayers in the liquid-ordered phase and sterol-free, pure DMPC bilayer, in the liquid-disordered phase). The results obtained indicate that although AmB dimers are formed in all of the environments studied, the dimerization process is less thermodynamically favorable in the Erg-rich liquid-ordered phase than in the Cho-rich liquid-ordered or pure liquid-disordered phases. We further investigate the possible molecular basis for this difference. We also compare the internal structure of the AmB dimers as well as their overall structural properties, such as the preferred location and orientation across three different membrane environments. The implications of our findings for the AmB mechanism of action are discussed.

METHODS

Molecular dynamics simulations

Molecular model

We studied head-to-head dimerization of AmB in lipid bilayers of various compositions:

1. Dimyristoylphosphatidylcholine (DMPC) membrane;
2. DMPC membrane with ~30 mol % of ergosterol (Erg); and
3. DMPC membrane with ~30 mol % of cholesterol (Cho).

These systems will be referred to as DMPC-Pure, DMPC/Erg, and DMPC/Cho, respectively. The initial structures of the bilayers were prepared using equilibrated configurations of sterol-containing DMPC bilayers taken from the previous MD simulations (8,10). The initial geometry of the AmB dimer was obtained from a systematic search procedure of the relative positions and orientations of the two AmB molecules as the lowest energy structure (for details of this procedure, see Neumann et al. (8)). In all three systems two neighboring DMPC molecules were removed from one of the bilayer leaflets and replaced by this energetically optimal AmB dimer, which has similar cross-sectional area (~56.0 $Å^2$ per AmB) (39) as compared to the experimental values for a pure DMPC bilayer and a 7:3 DMPC/Cho mixture (~60.0 $Å^2$ and ~45.0 $Å^2$ per DMPC, respectively) (40,41). The dimers were placed in a manner consistent with the putative mechanism of action of AmB, that is, with the AmB polar head (Fig. 1 *A*) located at the bilayer/water interface and the lactone ring buried within the membrane hydrocarbon core. The final model contained two membrane-embedded AmB molecules, 98 DMPC lipids (48 and 50 molecules per leaflet), 44 sterol molecules (in DMPC/Erg and DMPC/Cho), and 3256 water molecules.

Molecular dynamics simulations

All molecular dynamics (MD) simulations were performed with NAMD2.8 (42). The CHARMM36 lipid force field (43) used for the DMPC molecules allowed for the MD simulations to be performed in the tensionless isothermal-isobaric ensemble (NPT). The special set of parameters taken from Cournia et al. (44) and consistent with the CHARMM force field

was employed for the sterol molecules. As for the antibiotic molecule, the bonded and Lennard-Jones parameters were taken from the CHARMM22 library (45) and the partial charges were obtained by fitting to the quantum-mechanical electrostatic potential (46). The conformational properties of the AmB polar head calculated with this parameter set (10,47) showed to be consistent with both the AmB crystal structure (48) and the NMR data (49). The structure of AmB-sterol complexes as well as the higher affinity of AmB for Erg than for Cho (9,49) was also well reproduced (8,10). The TIP3P model was used for water. The atmospheric pressure was kept constant using the Langevin piston method (50). The temperature was maintained at 300 K by means of Langevin dynamics. Long-range electrostatic interactions were calculated using the particle-mesh Ewald method (51) with mesh size of ~1.0 Å and cubic interpolation. The Lennard-Jones potential and forces were smoothly switched off between 10 and 12 Å. Covalent bonds involving hydrogen atoms were constrained using the SHAKE algorithm (52), except for water, for which the SETTLE algorithm (53) was applied. This allowed for a time step of $\Delta t = 2$ fs to be used to integrate the equations of motion in the velocity Verlet algorithm. To test our models against the experimental data we computed the deuterium order parameter and the area per lipid for all three systems. The obtained values agree very well with the measured data (19,40,41) and show that the pure DMPC bilayer and the two sterol-containing bilayers are in liquid-disordered and liquid-ordered states, respectively (see Fig. S1, Fig. S2, and Table S1 in the Supporting Material). Importantly, the experimentally demonstrated difference between the latter two bilayers is also reproduced with the DMPC/Erg system showing a considerably higher conformational order and a tighter packing than the DMPC/Cho system.

Free energy calculations

The free energy profiles (potential of mean force, PMF) for the dimerization of AmB molecules in the three considered membrane environments were obtained using the adaptive biasing force (ABF) method (37,38). The reaction coordinate, ξ, for this process was defined as the distance separating the centers of mass (COM) of the two AmB molecules projected on the *xy* plane. In the ABF method the free energy is computed as an integral over ξ of the average force acting along the reaction coordinate. The sampling of the reaction coordinate is enhanced by applying biasing forces to the system that help to overcome free energy barriers. In ABF simulations these forces are computed as derivatives of continuously updated PMF. To further increase the efficiency of the calculation, the AmB-AmB association pathway, namely the interval $4.0 \leq \xi \leq 26.0$ Å, was divided into 21 equally sized windows. For each of these windows, 500 ns of MD trajectory was generated, which is longer than the characteristic time of most of the local dynamic processes that may affect the dimerization equilibrium in a lipid membrane (i.e., conformational changes, rotations, and local translations occur on a timescale <100 ns (54)). Instantaneous values of the force were accrued in 0.1 Å-wide bins. The standard error of the resulting free energy profiles was estimated using the expression given by Rodriguez-Gomez et al. (55). The initial structures for each window were obtained in the steered MD simulations, in which the AmB molecules forming a dimer are pulled away from each other in a bilayer plane with a constant velocity of 0.2 Å/ns up to the distance of 25 Å. Before the actual ABF simulations, the systems were allowed to relax for 10 ns with the distance between AmBs harmonically restrained to keep ξ around the center of a given window.

RESULTS AND DISCUSSION

Free energy profiles for AmB dimerization

To determine the tendency to form head-to-head AmB dimers in lipid bilayers containing or not physiological concentrations of Erg or Cho, we calculated the free energy profiles (PMFs) along the reaction coordinate ξ, defined as the distance between two AmB molecules projected on the bilayer plane, i.e., *xy* distance (Fig. 2). Such a reaction coordinate is expected to properly describe the association of two elongated AmB molecules, whose equilibrium mobility is limited by a lipid environment to translations in the *xy* plane and to rotations around the *z* axis. All the resulting PMFs are well converged as indicated by the small standard errors and by the convergence of the profiles with increasing simulation time (see Fig. S3).

Fig. 2 shows a large difference between the PMFs for the AmB dimerization process in the DMPC/Erg bilayer and in the DMPC/Cho or DMPC-Pure bilayers. Although AmB dimerization is favorable in all three systems (as indicated by the negative free energy values for bound configurations, i.e., small ξ-values, relative to 0 arbitrarily chosen for the unbound configurations), the bound substate is less favorable in the bilayer with Erg than in the Cho-containing or sterol-free ones. Not only is the PMF profile for DMPC/Erg more flat, with −4.0 kcal/mol at the minimum compared to −8 kcal/mol for DMPC/Cho and −7.3 kcal/mol for DMPC-Pure, but the minimum is also shifted toward larger distances. Indeed, the optimal distance between the two aggregating AmB molecules is 7.5 Å in DMPC/Erg and 6.1 Å in DMPC/Cho and DMPC-Pure. Thus, the equilibrium in the former case is shifted toward more loose AmB-AmB complexes. This is consistent with the solid-state NMR data (36) showing that the average intermolecular distance between the neighboring AmB molecules, measured as the separation between the labeled C42 and C46 atoms (Fig. 1 *A*), is increased in Erg-containing membranes by 2 Å relative to Cho-containing or sterol-free membranes. For direct comparison with these results, we first calculated the average distances between the two labeled atoms as a function of the reaction coordinate ξ. The equilibrium distances in the dimeric state, which were then obtained as a weighted average using $\exp(-\mathrm{PMF}(\xi)/k_B T)$ as

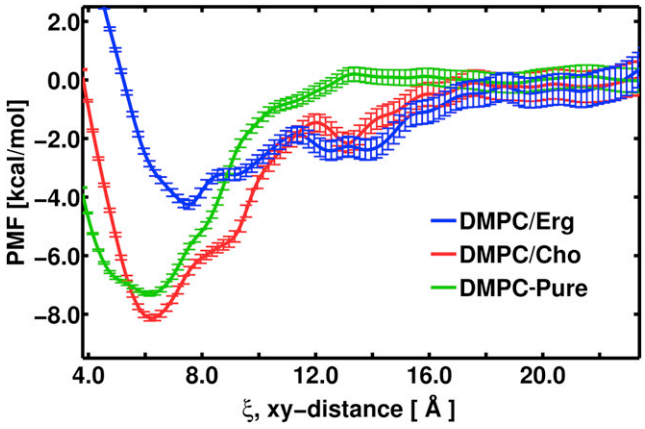

FIGURE 2 Free energy profiles (PMFs) along the reaction coordinate, ξ, defined as the distance separating the centers of mass of two AmB molecules projected on the *xy* plane (*xy* distance).

the weighting factor, showed similar shift as in the experiment (1.7 and 1.3 Å for DMPC/Cho and DMPC-Pure, respectively).

The smoothness of the free energy profiles in Fig. 2 differs due to different lipid packing around the AmB molecule in the three considered membranes. The lack of a packing pattern in the least conformationally ordered DMPC-Pure bilayer (liquid-disordered state; see Fig. S1 for the order parameter profiles) results in the smoothest PMF with only one well-pronounced minimum corresponding to a dimer of two directly interacting AmB molecules. In contrast, for both sterol-containing membranes (liquid-ordered state; see Fig. S1), tighter packing and enhanced spatial correlations between the bilayer constituents are reflected in the fine structure of the profiles. A second, less pronounced minimum observed for these systems at ~13.0 Å corresponds to a more loosely bound dimer mediated either by a highly ordered DMPC molecule or by a sterol molecule.

Dimerization equilibrium

To gain a more detailed insight into the thermodynamics of AmB self-association in a lipid bilayer, from the PMFs we calculated the dimerization free energies, $\Delta G = -k_B T \ln K$, where equilibrium constant $K = \int_b \rho(\xi) d\xi / \int_u \rho(\xi) d\xi$ and $\rho(\xi) = (2\pi\xi \exp(-\mathrm{PMF}(\xi)/k_B T))$. The b and u symbols denote the integration over the bound and unbound substates, respectively. Table 1 presents ΔG values calculated for a standard state imposed by the simulation conditions (the upper integration limit for unbound substate was set to 25 Å, which is less than half of the shorter lateral dimension of the bilayer). The results show that association of two AmB molecules in Cho-containing and sterol-free membranes is >4 kcal/mol more favorable than in one with Erg. This difference decreases slightly if we allow also the loosely bound dimers described by the second minimum that in the more ordered Erg-containing system is more pronounced than in the DMPC/Cho system.

To relate our results more directly to experimental data on the mechanism of AmB selectivity for Erg-containing membranes, we used the predicted equilibrium constants K to calculate the extent of the antibiotic dimerization in the three considered membrane systems. The computed extent of dimerization is presented in Fig. 3 as a function of the AmB/DMPC molar ratio ($R_{A/L}$). The resulting plots suggest that at low, chemotherapeutically relevant concentrations at which AmB expresses its channel-forming activity ($R_{A/L} \approx 10^{-4}$–10^{-3}) (3,56), the percentage of dimerized antibiotic molecules strongly depends on the membrane composition. According to our results, in this concentration range, AmB is mostly monomeric in Erg-containing membranes and it exists predominantly as a dimer in Cho-containing (and sterol-free) ones.

The dimerization free energy profiles indicate further that the lifetime of AmB dimers also depends on the type of sterol present in the bilayer. To quantify this, we used a simple formula for the dimer dissociation rate constant $k_{off} = \nu \exp(-\Delta G^{\neq}/k_B T)$. The activation barrier $\Delta G^{\neq}$ was taken from the PMFs. The frequency prefactor ν was estimated from the autocorrelation of xy distance, computed from the additional 500-ns equilibrium simulations of membrane-embedded AmB dimers (for DMPC/Erg and DMPC/Cho, $\nu \approx 0.06$ ns^{-1}). The average lifetime of the tight AmB dimers, k_{off}^{-1}, in the Cho-containing bilayer was found to be 1.5×0.10^3 μs, which is three orders of magnitude longer than the value of 1.2 μs for the bilayer with Erg.

It can be suggested that, with the AmB polyol chains involved in the formation of thermodynamically and kinetically stable dimers (Fig. 4), the availability of amphiphilic forms of AmB (such as the AmB monomers and the AmB-sterol complexes) is reduced. These species can be expected to be more effective in forming functional ion channels. Our results indicate that in the therapeutic range of concentrations, the pool of these monomeric AmBs is much greater in the Erg-containing bilayer compared to the Cho-containing one (Fig. 3). This may explain how the presence of Erg shifts the aggregation equilibrium toward the formation of

TABLE 1 Dimerization free energies, ΔG (in kcal/mol)

	Tight		Tight + loose	
	ξ' [Å]	ΔG	ξ' [Å]	ΔG
DMPC/Erg	11.3	−1.1 ± 0.39	15.5	−2.3 ± 0.50
DMPC/Cho	12.0	−5.2 ± 0.39	15.8	−6.1 ± 0.51
DPMC-Pure	13.5	−5.5 ± 0.36	—	—

Two different types of a bound substate were considered: tight, which includes only the first, most-pronounced minimum; and tight + loose, which includes also the second minimum. ξ' separates the bound and unbound substates. It differs among the three membranes due to the different location of the minima. Loosely bound dimers were not observed for DMPC-Pure (no second minimum).

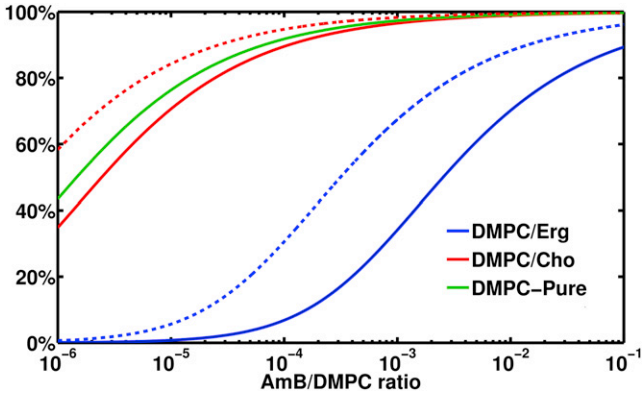

FIGURE 3 Extent of the antibiotic dimerization (ratio of the number of AmB molecules in dimeric form to the total number of AmBs) as a function of the AmB to DMPC concentration ratio (*solid lines*). (*Dashed lines*) The same, but with the loosely bound AmB dimers included in DMPC/Erg and DMPC/Cho.

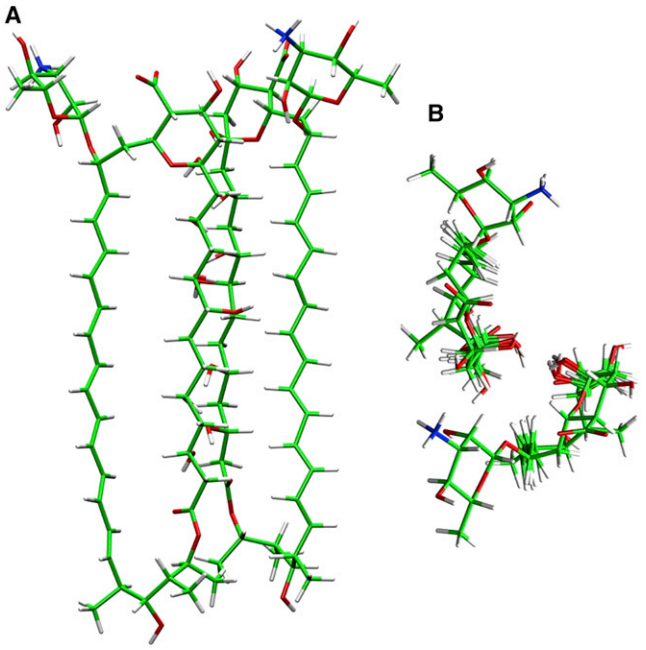

FIGURE 4 Typical structure of the head-to-head AmB dimer: side view (*A*) and top view as seen from the aqueous phase (*B*).

channel and, therefore, justify the higher activity of AmB against the Erg-rich membranes. From this perspective, strong interactions between AmB and membrane constituents (including specific AmB complexes with sterols), which prevent the initial aggregation into stable dimers, may also influence the increased membrane-permeabilizing activity of AmB.

In sterol-free membranes, as it follows from Fig. 3, AmB molecules dimerize to similar extent as in DMPC/Cho. However, as we discuss further, the experimentally established lower pore-forming activity of AmB in the sterol-free environment (3) might be a result of specific orientation and structure the dimers adopt in the liquid-disordered membrane phase (see the Structural Properties of AmB Dimers, below).

Molecular determinants of AmB dimerization

To fully understand the mechanism underlying the membrane activity of AmB, it is important to explain differences in the propensity of the antibiotic to form dimers in the three considered membranes, in particular to determine how the presence of ergosterol destabilizes the AmB dimers. To address this question, we first looked at how various contributions to the dimerization energies vary along the reaction coordinate. The computed contributions indicate that the energetics of the AmB dimerization process is largely dominated by the intradimer interactions between the AmB molecules as well as the local interactions between the AmB molecules and their immediate membrane environment (Fig. 5 and Fig. 6, and see Fig. S4). More global interactions, such as membrane-water or water-water, do not seem to contribute significantly to the differences among the three PMFs because the corresponding energies are the same (within the estimated uncertainty) for the bound and unbound substates.

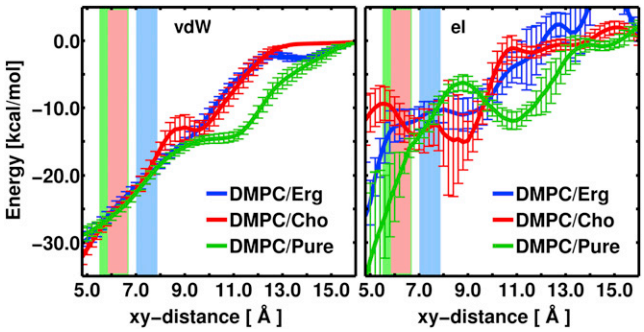

FIGURE 5 Interaction energy between the AmB molecules as a function of the *xy* distance between them. Van der Waals (vdW) and electrostatic interaction (el) contributions to the energy are considered separately. (*Shaded areas*) Width and location of the respective PMF minima (Fig. 2). The presented energies were averaged in ξ-bins and the uncertainties were calculated as the standard errors of the mean corrected for time-series correlation.

From the calculated data (Figs. 5 and 6), it is clear that the major determinant of the dimerization process, which compensates for the usual entropic penalty associated with bringing the two AmB molecules together (~0.8 kcal/mol for our standard state), is the electrostatic interaction between the dimerizing AmB molecules. The significant energy gain results mostly from the emerging interactions between the AmB polyol chains, i.e., C1–C13 in Fig. 1 *A* and not between the AmB polar heads, i.e., mycosamine

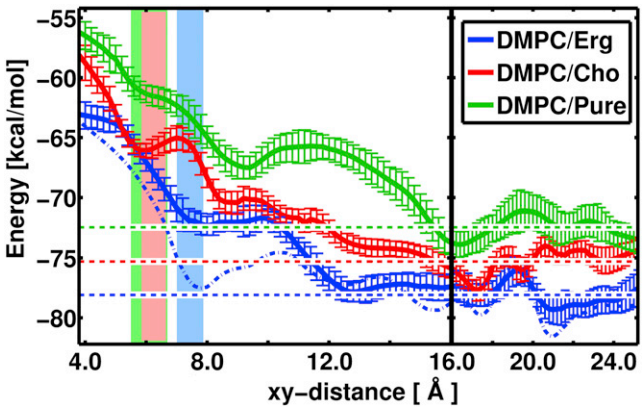

FIGURE 6 Energy of van der Waals interactions between AmB molecule and the hydrophobic membrane core as a function of the reaction coordinate ξ (the *xy* distance between the two dimerizing AmB molecules). The presented energies (*solid lines*) were averaged in ξ-bins and over two AmB molecules and the uncertainties were calculated as the standard errors of the mean corrected for time-series correlation. For DMPC/Erg the interaction energy for the selected, strongly interacting AmB molecule is shown separately (*dash-dot line*). (*Dashed horizontal lines*) Average interaction energy for monomeric AmB ($\xi > 16$ Å). (*Shaded areas*) Width and location of the respective PMF minima.

and carboxyl moieties (see also the analysis of hydrogen bonds in the Structural Properties of AmB Dimers, below). The polar heads are strongly engaged in interactions with the hydrophilic region of the membrane to similar extents in the bound and unbound states. The van der Waals AmB-AmB and AmB-membrane contributions largely cancel each other out.

The energetic decomposition further suggests that the main cause of the lower stability and of the more loose structure of the AmB dimers in the DMPC/Erg system is the nature of the interactions between AmB and a lipid matrix. Because the differences in the structural properties (e.g., the conformational order, see Fig. S1) of the three considered membranes are found mainly in the hydrophobic core (22,57), in Fig. 6 we show the interaction energy between AmB and this hydrocarbon region only. As can be seen in Fig. 5, to maximize the energy gain due to the AmB-AmB interaction, a close contact between the molecules at a distance of ~6 Å is required. However, as indicated in Fig. 6, the AmB monomers embedded in the most densely packed DMPC/Erg system interact most strongly with the hydrophobic core, either through close contacts with highly ordered lipid acyl chains or by forming specific complexes with Erg molecules (as previously shown in Neumann et al. (10)). Therefore, for the dimer in DMPC/Erg, the optimal distance ξ between the AmB molecules is not ~6 Å but ~8 Å, a distance that characterizes a more loosely bound complex in which AmB molecules are still able to interact strongly with membrane constituents (Fig. 6). Especially for one AmB in this system, remaining relatively perpendicular to the bilayer plane (see Fig. S5), the transition from $\xi \approx 8$ Å to $\xi \approx 6$ Å is associated with an abrupt truncation of these very favorable interactions (*dash-dot line* in Fig. 6). In the less-ordered bilayers (DMPC/Cho, DMPC-Pure, see Fig. S1) the interactions between the AmB monomer and the membrane are weaker, enabling the AmB molecules to maximize their mutual interaction at the optimal distance of ~6 Å. The less ordered environment makes it easier for the AmB molecules to tilt (see Fig. S5) and, thus, in DMPC/Cho and especially in DMPC-Pure, the AmB-membrane interactions are replaced by AmB-AmB interactions more gradually with the decreasing distance.

One might expect that association of two AmB molecules in a membrane environment causes change in the lipid packing arrangement, especially in the vicinity of the dimerizing molecules. As a result of different packing properties (see Table S1), these changes may vary among the three considered bilayers and, therefore, may differently affect the energetics of the dimerization process. The procedure that we used to compare the dimerization-induced changes in lipid packing among the three systems and the resulting data are described in detail in the Supporting Material. The results indicate that the self-association of AmBs in the most ordered and tightly packed membrane may disrupt the network of interactions between lipid acyl chains and may disturb the hexatic packing of the highly ordered lipid phases. This hypothesis was tested and the results demonstrate that considerable decrease in the quality of the hydrophobic core packing due to the AmB dimerization is observed in the Erg-containing bilayer, with no such effect for the two remaining systems. Thus, it seems that, compared to the dimer, the monomer of AmB fits more naturally into a tightly packed membrane with Erg and, consequently, that the lipid-lipid interactions appear to hinder the dimer formation in the DMPC/Erg membrane.

Structural properties of AmB dimers

Differences in molecular architecture of AmB self-aggregates are often considered to account for the diverse activity of the antibiotic against lipid membranes of different composition (7,27). Therefore, it was interesting to examine whether and how the membrane environment affects the structure of AmB dimers, in particular whether the observed differences in the dimer stability correspond to different structural behavior of these aggregates across the three considered membrane environments.

Fig. 7 shows the optimal mutual arrangement of the two AmB molecules at a distance corresponding to the dimer formation in the DMPC/Erg and DMPC/Cho bilayers. As expected, in both environments, the polar polyol chains are held together and the hydrophobic polyene fragments are exposed to the membrane hydrocarbon core (see also Fig. 4). Our simulations indicate, however, that the relative orientation of the AmB molecules in the dimer depends on the type of sterol present in the membrane. The AmB-AmB distance is larger (~8 Å) in DMPC/Erg, yet relative orientation of the two rigid macrolactone rings in this bilayer

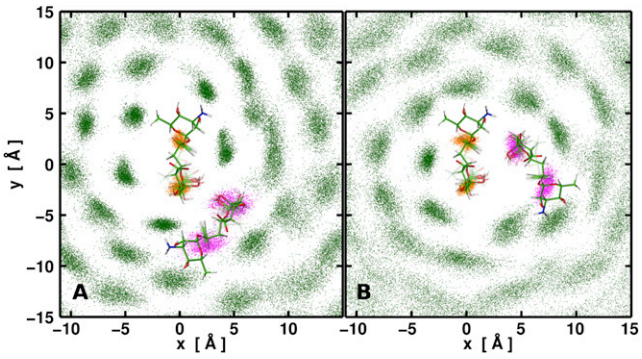

FIGURE 7 Packing of the hydrophobic core of the Erg-containing (*A*) and Cho-containing (*B*) membranes around AmB molecules at the optimal distance (7.5 and 6.1 Å in Erg- and Cho-containing membranes, respectively). The positional distributions of the lipid acyl chains and the sterol molecules around the AmB polyol and polyene chains were generated from ~50-ns-long trajectories (the maximal time throughout which the distance ξ is continuously close to the optimal). The coordinates of the points were defined as the *xy* coordinates of COMs of the selected molecular fragments (the more disordered C8–C14 parts of the acyl chains and the sterol side chains were excluded).

(Fig. 7 *A*) is more stable than in DMPC/Cho, where the more closely bound dimer (~6 Å) is more orientationally flexible (see Fig. S6). This orientational stability of the AmB dimer in DMPC/Erg is due to the above-described strong interactions between the associated antibiotic molecules and the membrane components. This is expressed in Fig. 7 *A* by a dense distribution of points representing the positions of the lipid acyl chains around the dimer. It is also important to note that in the here-proposed structure of the AmB dimers the polyene chains are separated by a distance of 8–12 Å (see also Fig. S7), the distance at which the interactions between these chromophores cannot be detected by UV-Vis spectroscopy. This might be the reason why previous spectroscopic studies did not directly demonstrate the distinctly different tendency of AmB to form this kind of self-aggregate for Erg- and Cho-containing bilayers and therefore this difference was not discussed in the context of the AmB selective toxicity.

To determine which structural elements of the AmB molecule are responsible for the driving force of the AmB dimerization, we investigated how the average number of hydrogen bonds between the selected polar groups of the antibiotic molecule varies with the distance, ξ, between them. As can be seen in Fig. 8 for the closely spaced dimer ($5 < \xi < 9$ Å), the pattern of AmB-AmB hydrogen bonds does not depend significantly on the membrane composition with the polyol-polyol and polyol-head interactions being much more pronounced than the head-head interactions in all three systems. The minor involvement of the AmB polar heads in dimer stabilization is rather surprising, because these moieties are often considered important for AmB self-association in a lipid bilayer (58,59). This may also indicate that certain covalent modifications of the AmB polar head that improve the antibiotic selectivity (60–62) and, as we have recently proposed, lead to the increased affinity of the antibiotic for Erg (and not for Cho) (10), should not largely affect the stability of the dimer. Therefore, by strengthening the AmB-membrane interactions (by encouraging the AmB-Erg complexes formation), these modifications could further shift the dimerization equilibrium in the DMPC/Erg bilayer toward monomers, while having little effect on the dimer stability in DMPC/Cho. If, as suggested above, the monomers are the basic building blocks for the formation of a functional channel, this additional difference in the tendency to dimerize between DMPC/Cho and DMPC/Erg would more fully explain the increased selectivity for fungal membranes observed for the so-called second generation of AmB derivatives (60–63). To experimentally test the prediction that monomers are efficient substrates for the channel formation, one could substitute a selected hydroxyl group to prevent the formation of a hydrogen-bond network between the two polyols (e.g., with a small group that would not inhibit ion flux through a putative channel). This would strongly shift the equilibrium toward the monomeric state in all bilayers, which, according to our hypothesis, would decrease the selectivity for Erg-containing membranes.

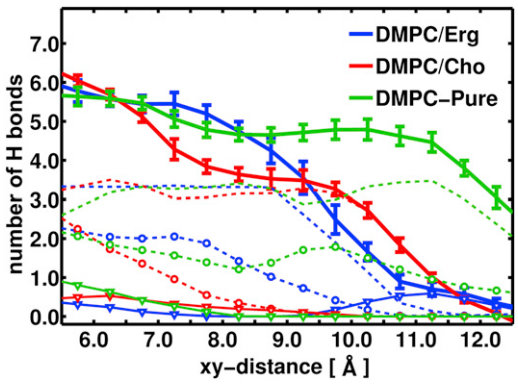

FIGURE 8 Average number of the intermolecular hydrogen bonds in the AmB dimer. The total number of hydrogen bonds (*solid lines* with *error bars*) was decomposed into bonds forming between the AmB polyols (*dashed lines*), between the AmB polar heads (*triangles*), and between the polyols and the polar heads (*circles*). Geometric hydrogen-bond criteria were used: D–A distance < 3.5 Å and D–H–A angle $> 120°$, where D = donor and A = acceptor.

Fig. 8 also shows that the less ordered the membrane environment, the easier it is for AmB molecules to tilt away from the normal to the membrane plane to form hydrogen bonds with each other. In the liquid-disordered phase (DMPC-Pure), some AmB-AmB contacts are formed between the two highly tilted molecules already at a distance of 13 Å, whereas in the liquid-ordered phases (DMPC/Erg and DMPC/Cho) the formation of strong hydrogen bonds begins at a distance of 10 Å. The distributions of the tilt angle shown in Fig. S5 as a function of the distance between the AmB molecules further confirm the mechanism of dimer formation in which, at intermediate distances, at least one AmB molecule tilts away from its equilibrium (relatively perpendicular) orientation to form hydrogen bonds with the partner. This effect is most pronounced in the most disordered sterol-free membrane, although it is also noticeable in the sterol-rich ordered phases.

To determine if the dimerization affects the position of AmB molecules within a membrane, we studied how the distance from the AmB's COM to the bilayer midplane depends on the *xy* distance between the dimerizing antibiotic molecules. The distributions shown in Fig. 9 indicate that, in sterol-containing membranes, AmB molecules reside in one leaflet of the bilayer with their polar heads located in the polar region of the membrane and the terminal C35 hydroxyl groups located approximately in the middle of the bilayer. The average equilibrium distance of the AmB's COM from the bilayer center is 14.0 Å in DMPC/Erg and 13.3 Å in DMPC/Cho, and does not vary significantly with the AmB-AmB separation distance.

Compared to the sterol-containing membranes, in the sterol-free membrane the mobility of the AmB molecules along the z axis is much less restricted and they can

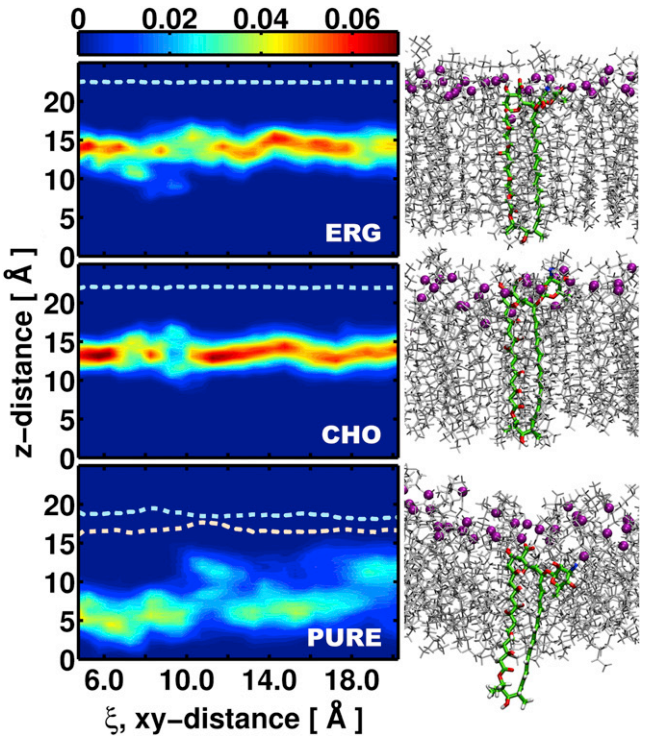

FIGURE 9 Distribution of the distance between the AmB's COM and the bilayer midplane as a function of the *xy* distance between the two antibiotic molecules (ξ). (*Dashed line*) Average position of DMPC phosphate groups (as a function of ξ), with all lipids taken into account for DMPC/Erg and DMPC/Cho and with lipids close to the AmB molecules (*lower line*) and far away from AmBs (*upper line*) presented separately for DMPC-Pure. The average z positions of the phosphate groups in DMPC/Erg and DMPC/Cho do not depend on the distance from AmB. Next to each distribution, a snapshot of the typical AmB position within the leaflet of the corresponding membrane is presented. (*Spheres*) Phosphorus atoms of DMPC molecules.

penetrate deeper into the hydrophobic core. In the sterol-free environment, the average equilibrium distance from the membrane midplane is 6.2 Å. However, with decreasing AmB-AmB distance, the antibiotic molecules shift further toward the center of the bilayer, such that in the dimeric state they are able to interact with the polar region of the opposite leaflet through the OH groups at C35 (each group forms on average 1.1 hydrogen bonds with water). Simultaneous interaction with the two polar regions reduces the positional fluctuation of the dimer along the membrane normal. It can be also seen that AmB deeply seated in the DMPC-Pure bilayer causes its local thinning: the structure of the DMPC-Pure bilayers adjusts locally to the presence of the AmB molecules by decreasing its thickness, measured as the average distance between phosphate groups, from 36 to 32 Å (Fig. 9).

The apparent difference in the location of AmB dimers within the sterol-containing and sterol-free membranes is consistent with earlier NMR data (64) showing that the self-associated form of AmB is able to span a relatively thin DMPC membrane but not a DSPC membrane whose thickness is similar to the thickness of the sterol-containing bilayers (~42 Å (65,66) vs. 45 and 44 Å for DMPC/Erg and DMPC/Cho, respectively). Therefore, it seems that both our results and the data of Matsuoka et al. (64) are consistent with the notion that the so-called double-length channels are formed within the relatively thick sterol-enriched liquid-ordered domains. This conclusion is also consistent with the recent finding that AmB analogs lacking the C35 hydroxyl group, presumably participating in the double-length channel stabilization, show much lower membrane-permeabilizing activity (12,13).

Despite the similarities between DMPC-Pure and DMPC/Cho in the overall tendency of AmB to dimerize and in the intrinsic structure of the AmB dimers, their position in the bilayer as well as their orientation with respect to bilayer plane are significantly different due to different properties of these two lipid environments. Thus, the lower activity of AmB against sterol-free membranes may result from the fact that the liquid-disordered membrane phase does not provide a suitable environment for AmB to aggregate to form functional channels. According to this hypothesis, to express its full membrane-permeabilizing activity, AmB requires the sterol-enriched membrane domains that provide a sufficiently densely packed and conformationally ordered environment for the channel formation.

CONCLUSIONS

As evidenced by the free energy profiles for AmB dimerization process, the head-to-head dimers of AmB are formed in all the systems studied, in the Erg- and Cho-containing as well as in the sterol-free lipid bilayers. The intermolecular interactions between AmB polyols are the major driving force for AmB dimer formation. These strong (mostly electrostatic and hydrogen-bond) interactions determine the structure of the AmB dimer in which the polyol chains are held together and the polyene segments are exposed to the membrane core. The relatively large distance between the polyene chromophores predicted by our simulations suggests that head-to-head AmB dimers may be difficult to detect and study by UV-Vis spectroscopy.

Despite structural similarities, the head-to-head dimers of AmB are much less favorable (thermodynamically) and less stable (kinetically) in the bilayer with Erg than in the Cho-containing one. The lower tendency of AmB to form dimers in the Erg-containing membrane causes that, at chemotherapeutically relevant concentrations, the monomeric form of the antibiotic is dominant in this bilayer. In the presence of ergosterol the optimal distance between two AmB molecules is increased by almost 2 Å, thus, more loose aggregates are formed, in agreement with the experimental results (36). The lower stability and the more loose structure of the AmB dimers in the DMPC/Erg system compared to DMPC/Cho is mostly due to the stronger interactions of the antibiotic with the membrane hydrophobic core. Indeed,

the AmB molecules interact most strongly with the most ordered bilayer, either by forming specific complexes with Erg molecules (10) or through close contacts with highly ordered and densely packed lipid acyl chains. Therefore, the different tendency of AmB to form dimers in DMPC/Erg and in DMPC/Cho revealed by our study is in agreement with the different affinity of AmB for both sterols (8,10), a phenomenon that was recently also suggested to underlie the antifungal effect of AmB unrelated to membrane permeabilization (13).

If one assumes that amphiphilic AmB species (such as monomers or AmB-sterol complexes) are more likely to form ion channels, then burying polyol chains inside thermodynamically and kinetically stable dimers might reduce the pore-forming action. From this perspective, strong interactions between AmB and membrane constituents, which prevent the initial aggregation into stable dimers, may also influence the increased membrane-permeabilizing activity of AmB.

Although the head-to-head AmB dimers are formed also in the sterol-free bilayer, it is known that in this bilayer the membrane-disrupting effect of AmB is diminished and requires higher concentrations of the antibiotic (3,7). This, together with our observation that AmB molecules in both (monomeric and self-aggregated) forms have a low orientational and positional stability in the sterol-free disordered bilayer, suggest that an ordered lipid environment can be regarded as favorable for the formation of stable channels.

SUPPORTING MATERIAL

Eight figures and one table are available at http://www.biophysj.org/biophysj/supplemental/S0006-3495(13)00247-6.

The authors thank Academic Computer Centre TASK (Gdansk, Poland) and Cyfronet (Krakow, Poland) computational centers for granting CPU time.

This research was supported in part by PL-Grid Infrastructure. This work was supported by Polish National Science Centre grant No. N519657440.

REFERENCES

1. Hann, I. M., and H. G. Prentice. 2001. Lipid-based amphotericin B: a review of the last 10 years of use. *Int. J. Antimicrob. Agents.* 17:161–169.
2. Moen, M. D., K. A. Lyseng-Williamson, and L. J. Scott. 2009. Liposomal amphotericin B: a review of its use as empirical therapy in febrile neutropenia and in the treatment of invasive fungal infections. *Drugs.* 69:361–392.
3. Bolard, J. 1986. How do the polyene macrolide antibiotics affect the cellular membrane properties? *Biochim. Biophys. Acta.* 864:257–304.
4. Baginski, M., and J. Czub. 2009. Amphotericin B and its new derivatives—mode of action. *Curr. Drug Metab.* 10:459–469.
5. Hartsel, S., and J. Bolard. 1996. Amphotericin B: new life for an old drug. *Trends Pharmacol. Sci.* 17:445–449.
6. Vertut-Croquin, A., J. Bolard, …, C. Gary-Bobo. 1983. Differences in the interaction of the polyene antibiotic amphotericin B with cholesterol- or ergosterol-containing phospholipid vesicles. A circular dichroism and permeability study. *Biochemistry.* 22:2939–2944.
7. Huang, W. M., Z. L. Zhang, …, E. Wang. 2002. Ion channel behavior of amphotericin B in sterol-free and cholesterol- or ergosterol-containing supported phosphatidylcholine bilayer model membranes investigated by electrochemistry and spectroscopy. *Biophys. J.* 83:3245–3255.
8. Neumann, A., J. Czub, and M. Baginski. 2009. On the possibility of the amphotericin B-sterol complex formation in cholesterol- and ergosterol-containing lipid bilayers: a molecular dynamics study. *J. Phys. Chem. B.* 113:15875–15885.
9. Matsumori, N., K. Tahara, …, M. Murata. 2009. Direct interaction between amphotericin B and ergosterol in lipid bilayers as revealed by ^{2}H NMR spectroscopy. *J. Am. Chem. Soc.* 131:11855–11860.
10. Neumann, A., M. Baginski, and J. Czub. 2010. How do sterols determine the antifungal activity of amphotericin B? Free energy of binding between the drug and its membrane targets. *J. Am. Chem. Soc.* 132:18266–18272.
11. de Kruijff, B., and R. A. Demel. 1974. Polyene antibiotic-sterol interactions in membranes of *Acholeplasma laidlawii* cells and lecithin liposomes. 3. Molecular structure of the polyene antibiotic-cholesterol complexes. *Biochim. Biophys. Acta.* 339:57–70.
12. Palacios, D. S., I. Dailey, …, M. D. Burke. 2011. Synthesis-enabled functional group deletions reveal key underpinnings of amphotericin B ion channel and antifungal activities. *Proc. Natl. Acad. Sci. USA.* 108:6733–6738.
13. Gray, K. C., D. S. Palacios, …, M. D. Burke. 2012. Amphotericin primarily kills yeast by simply binding ergosterol. *Proc. Natl. Acad. Sci. USA.* 109:2234–2239.
14. Cotero, B. V., S. Rebolledo-Antunez, and I. Ortega-Blake. 1998. On the role of sterol in the formation of the amphotericin B channel. *Biochim. Biophys. Acta Biomembr.* 1375:43–51.
15. Venegas, B., J. González-Damián, …, I. Ortega-Blake. 2003. Amphotericin B channels in the bacterial membrane: role of sterol and temperature. *Biophys. J.* 85:2323–2332.
16. Coutinho, A., L. Silva, …, M. Prieto. 2004. Cholesterol and ergosterol influence nystatin surface aggregation: relation to pore formation. *Biophys. J.* 87:3264–3276.
17. Ostroumova, O. S., S. S. Efimova, and L. V. Schagina. 2012. Probing amphotericin B single channel activity by membrane dipole modifiers. *PLoS ONE.* 7:e30261.
18. Ostroumova, O. S., S. S. Efimova, …, L. V. Schagina. 2012. The interaction of dipole modifiers with polyene-sterol complexes. *PLoS ONE.* 7:e45135.
19. Urbina, J. A., S. Pekerar, …, E. Oldfield. 1995. Molecular order and dynamics of phosphatidylcholine bilayer membranes in the presence of cholesterol, ergosterol and lanosterol: a comparative study using ^{2}H-, ^{13}C- and ^{31}P-NMR spectroscopy. *Biochim. Biophys. Acta Biomembr.* 1238:163–176.
20. Miao, L., M. Nielsen, …, O. G. Mouritsen. 2002. From lanosterol to cholesterol: structural evolution and differential effects on lipid bilayers. *Biophys. J.* 82:1429–1444.
21. Hsueh, Y. W., K. Gilbert, …, J. Thewalt. 2005. The effect of ergosterol on dipalmitoylphosphatidylcholine bilayers: a deuterium NMR and calorimetric study. *Biophys. J.* 88:1799–1808.
22. Czub, J., and M. Baginski. 2006. Comparative molecular dynamics study of lipid membranes containing cholesterol and ergosterol. *Biophys. J.* 90:2368–2382.
23. Aracava, Y., S. Schreier, …, I. C. Smith. 1981. Effects of amphotericin B on membrane permeability—kinetics of spin probe reduction. *Biophys. Chem.* 14:325–332.
24. Dufourc, E. J., I. C. Smith, and H. C. Jarrell. 1984. Amphotericin and model membranes. The effect of amphotericin B on cholesterol-containing systems as viewed by ^{2}H-NMR. *Biochim. Biophys. Acta.* 776:317–329.
25. Czub, J., and M. Baginski. 2006. Modulation of amphotericin B membrane interaction by cholesterol and ergosterol—a molecular dynamics study. *J. Phys. Chem. B.* 110:16743–16753.

26. Fournier, I., J. Barwicz, …, P. Tancrède. 2008. The chain conformational order of ergosterol- or cholesterol-containing DPPC bilayers as modulated by amphotericin B: a FTIR study. *Chem. Phys. Lipids.* 151:41–50.

27. Bolard, J., P. Legrand, …, B. Cybulska. 1991. One-sided action of amphotericin B on cholesterol-containing membranes is determined by its self-association in the medium. *Biochemistry.* 30:5707–5715.

28. Hing, A. W., J. Schaefer, and G. S. Kobayashi. 2000. Deuterium NMR investigation of an amphotericin B derivative in mechanically aligned lipid bilayers. *Biochim. Biophys. Acta Biomembr.* 1463:323–332.

29. Lopes, S., and M. A. R. B. Castanho. 2002. Revealing the orientation of nystatin and amphotericin B in lipidic multilayers by UV-Vis linear dichroism. *J. Phys. Chem. B.* 106:7278–7282.

30. Gruszecki, W. I., M. Gagoś, and M. Hereć. 2003. Dimers of polyene antibiotic amphotericin B detected by means of fluorescence spectroscopy: molecular organization in solution and in lipid membranes. *J. Photochem. Photobiol. B.* 69:49–57.

31. Gagoś, M., and M. Arczewska. 2010. Spectroscopic studies of molecular organization of antibiotic amphotericin B in monolayers and dipalmitoylphosphatidylcholine lipid multibilayers. *Biochim. Biophys. Acta Biomembr.* 1798:2124–2130.

32. Umegawa, Y., N. Matsumori, …, M. Murata. 2007. Amphotericin B covalent dimers with carbonyl-amino linkage: a new probe for investigating ion channel assemblies. *Tetrahedron Lett.* 48:3393–3396.

33. Umegawa, Y., T. Adachi, …, M. Murata. 2012. Possible conformation of amphotericin B dimer in membrane-bound assembly as deduced from solid-state NMR. *Bioorg. Med. Chem.* 20:5699–5704.

34. Caillet, J., J. Bergés, and J. Langlet. 1995. Theoretical study of the self-association of amphotericin B. *Biochim. Biophys. Acta.* 1240:179–195.

35. Mazerski, J., and E. Borowski. 1996. Molecular dynamics of amphotericin B. II. Dimer in water. *Biophys. Chem.* 57:205–217.

36. Umegawa, Y., N. Matsumori, …, M. Murata. 2008. Ergosterol increases the intermolecular distance of amphotericin B in the membrane-bound assembly as evidenced by solid-state NMR. *Biochemistry.* 47:13463–13469.

37. Darve, E., and A. Pohorille. 2001. Calculating free energies using average force. *J. Chem. Phys.* 115:9169–9183.

38. Hénin, J., and C. Chipot. 2004. Overcoming free energy barriers using unconstrained molecular dynamics simulations. *J. Chem. Phys.* 121:2904–2914.

39. Saint-Pierre-Chazalet, M., C. Thomas, …, C. M. Gary-Bobo. 1988. Amphotericin B-sterol complex formation and competition with egg phosphatidylcholine: a monolayer study. *Biochim. Biophys. Acta.* 944:477–486.

40. Hung, W. C., M. T. Lee, …, H. W. Huang. 2007. The condensing effect of cholesterol in lipid bilayers. *Biophys. J.* 92:3960–3967.

41. Pan, J., S. Tristram-Nagle, and J. F. Nagle. 2009. Effect of cholesterol on structural and mechanical properties of membranes depends on lipid chain saturation. *Phys. Rev. E Stat. Nonlin. Soft Matter Phys.* 80: 021931.

42. Kale, L., R. Skeel, …, K. Schulten. 1999. NAMD2: greater scalability for parallel molecular dynamics. *J. Comput. Phys.* 151:283–312.

43. Klauda, J. B., R. M. Venable, …, R. W. Pastor. 2010. Update of the CHARMM all-atom additive force field for lipids: validation on six lipid types. *J. Phys. Chem. B.* 114:7830–7843.

44. Cournia, Z., J. C. Smith, and G. M. Ullmann. 2005. A molecular mechanics force field for biologically important sterols. *J. Comput. Chem.* 26:1383–1399.

45. Baginski, M., H. Resat, and E. Borowski. 2002. Comparative molecular dynamics simulations of amphotericin B-cholesterol/ergosterol membrane channels. *Biochim. Biophys. Acta Biomembr.* 1567:63–78.

46. Baginski, M., and E. Borowski. 1997. Distribution of electrostatic potential around amphotericin B and its membrane targets. *J. Mol. Struct. Theochem.* 389:139–146.

47. Czub, J., A. Neumann, …, M. Baginski. 2009. Influence of a lipid bilayer on the conformational behavior of amphotericin B derivatives—a molecular dynamics study. *Biophys. Chem.* 141:105–116.

48. Ganis, P., G. Avitabile, …, C. P. Schaffner. 1971. Polyene macrolide antibiotic amphotericin B. Crystal structure of the *n*-iodoacetyl derivative. *J. Am. Chem. Soc.* 93:4560–4564.

49. Matsumori, N., Y. Sawada, and M. Murata. 2005. Mycosamine orientation of amphotericin B controlling interaction with ergosterol: sterol-dependent activity of conformation-restricted derivatives with an amino-carbonyl bridge. *J. Am. Chem. Soc.* 127:10667–10675.

50. Feller, S. E., Y. Zhang, …, B. R. Brooks. 1995. Constant pressure molecular dynamics simulation: the Langevin piston method. *J. Chem. Phys.* 103:4613–4621.

51. Darden, T., D. York, and L. Pedersen. 1993. Particle mesh Ewald: an *N*log(*N*) method for Ewald sums in large systems. *J. Chem. Phys.* 98:10089–10092.

52. Ryckaert, J. P., G. Cicotti, and H. J. C. Berendsen. 1977. Numerical integration of the Cartesian equations of motion of a system with constraints: molecular dynamics of *n*-alkanes. *J. Comput. Phys.* 23: 327–341.

53. Miyamoto, S., and P. A. Kollman. 1992. SETTLE: an analytical version of the SHAKE and RATTLE algorithm for rigid water models. *J. Comput. Chem.* 13:952–962.

54. Pastor, R. W., R. M. Venable, and S. E. Feller. 2002. Lipid bilayers, NMR relaxation, and computer simulations. *Acc. Chem. Res.* 35: 438–446.

55. Rodriguez-Gomez, D., E. Darve, and A. Pohorille. 2004. Assessing the efficiency of free energy calculation methods. *J. Chem. Phys.* 120: 3563–3578.

56. Fujii, G., J. E. Chang, …, B. Steere. 1997. The formation of amphotericin B ion channels in lipid bilayers. *Biochemistry.* 36:4959–4968.

57. Brown, M. F., and J. Seelig. 1978. Influence of cholesterol on the polar region of phosphatidylcholine and phosphatidylethanolamine bilayers. *Biochemistry.* 17:381–384.

58. Cybulska, B., M. Herve, …, C. M. Gary-Bobo. 1986. Effect of the polar head structure of polyene macrolide antifungal antibiotics on the mode of permeabilization of ergosterol- and cholesterol-containing lipidic vesicles studied by ^{31}P-NMR. *Mol. Pharmacol.* 29:293–298.

59. Herve, M., J. C. Debouzy, …, C. M. Gary-Bobo. 1989. The role of the carboxyl and amino groups of polyene macrolides in their interactions with sterols and their selective toxicity. A ^{31}P-NMR study. *Biochim. Biophys. Acta.* 980:261–272.

60. Borowski, E. 2000. Novel approaches in the rational design of antifungal agents of low toxicity. *Farmaco.* 55:206–208.

61. Szlinder-Richert, J., J. Mazerski, …, E. Borowski. 2001. MFAME, N-methyl-*n*-D-fructosyl amphotericin B methyl ester, a new amphotericin B derivative of low toxicity: relationship between self-association and effects on red blood cells. *Biochim. Biophys. Acta.* 1528:15–24.

62. Slisz, M., B. Cybulska, …, E. Borowski. 2007. The mechanism of overcoming multidrug resistance (MDR) of fungi by amphotericin B and its derivatives. *J. Antibiot.* 60:436–446.

63. Czub, J., E. Borowski, and M. Baginski. 2007. Interactions of amphotericin B derivatives with lipid membranes—a molecular dynamics study. *Biochim. Biophys. Acta Biomembr.* 1768:2616–2626.

64. Matsuoka, S., H. Ikeuchi, …, M. Murata. 2005. Dominant formation of a single-length channel by amphotericin B in dimyristoylphosphatidylcholine membrane evidenced by ^{13}C-^{31}P rotational echo double resonance. *Biochemistry.* 44:704–710.

65. Lewis, B. A., and D. M. Engelman. 1983. Lipid bilayer thickness varies linearly with acyl chain length in fluid phosphatidylcholine vesicles. *J. Mol. Biol.* 166:211–217.

66. Nagle, J. F., and S. Tristram-Nagle. 2000. Structure of lipid bilayers. *Biochim. Biophys. Acta Biomembr.* 1469:159–195.